

Received 26 February 2023, accepted 20 March 2023, date of publication 3 August 2023, date of current version 17 August 2023.

Digital Object Identifier 10.1109/ACCESS.2023.3301567



# Interactive Occlusion-Free System for Accessible Volume Exploration

JING-RU SUN, NATHANIA JOSEPHINE, CHAO WANG<sup>✉</sup>, (Member, IEEE),

AND KO-CHIH WANG<sup>✉</sup>, (Member, IEEE)

Department of Computer Science and Information Engineering, National Taiwan Normal University, Taipei 11677, Taiwan

Corresponding author: Ko-Chih Wang (kewang@ntnu.edu.tw)

This work was supported in part by the National Science and Technology Council (NSTC) of Taiwan: Deep Learning-Based In-Situ Scientific Data Visualization and Analysis under Grant 109-2222-E-003-002-MY3, and in part by the Distribution-Based Data Reduction for Query-Based Analysis and Visualization of Large Time-Varying Ensemble Datasets under Grant 111-2221-E-003-015-MY3.

**ABSTRACT** When exploring a 3D medical dataset, data occlusion creates difficulties for users to understand the dataset in detail since many internal structures are occluded. Techniques such as transfer function design, isosurface extraction, etc., have been proposed in the past to address the occlusion problem and assist expert users in exploring volumetric data. However, these techniques may not be feasible for some non-expert users' scenarios, such as science museum visitors exploring a brain CT image data volume on a large touch screen or high school students learning the human body structure on a tablet because they have no need to conduct long-term data exploration and rigorous scientific analysis. To address the non-expert users' need for an easy-to-use data exploration tool, we propose an interactive data exploration system for non-expert users to interact with the dataset with a short learning time and simple inputs. Non-expert users can remove the obstructing material to reveal the occluded structures by simply clicking on the obstructing material. Our system also preserves the context for non-expert users to understand the dataset after the obstructing material is removed easily. Additionally, for data providers such as the engineers in a museum, our system provides a semi-automatic workflow to set up a dataset into our system for non-expert users. In this work, we conduct two user studies to evaluate our system's usability.

**INDEX TERMS** 3D data visualization and exploration, human–computer interaction, occlusion management.

## I. INTRODUCTION

Volume visualization [1] is a major technique that assists users in comprehending complex geometric structures of three-dimensional space. The technique has been widely used in engineering, architecture, medicine, and other scientific fields. For instance, experienced physicians can review computed tomography (CT) and magnetic resonance imaging (MRI) scans to diagnose and make decisions for surgery. Data occlusion creates difficulties for users to explore and understand a 3D dataset in detail since many of the details are occluded when the dataset is rendered on the 2D screen. In order to assist users in exploring 3D datasets, many techniques have been invented in the past few decades. For

The associate editor coordinating the review of this manuscript and approving it for publication was Alessandro Floris<sup>✉</sup>.

example, transfer function is designed to define the colors and opacities of different data materials to project 3D dataset to 2D screen space [2], [3], [4]; Isosurface extraction [5] is used to retrieve the surface with the same data value giving experts the ability to observe the specific geometric shapes to identify important features of the datasets; Data removal or data deformation techniques [6], [7], [8], [9] allow experts to remove obstruction between the view and the feature of interest. Although these techniques can help experts explore their datasets, they may not be feasible for non-experts. For example, science museum visitors exploring a brain CT image volume dataset on a large touch screen or high school students learning the human body structure by interacting with the data on a tablet are both non-expert user scenarios. These non-expert users usually do not have a long time to interact with the dataset and conduct rigorous scientific studies, and they

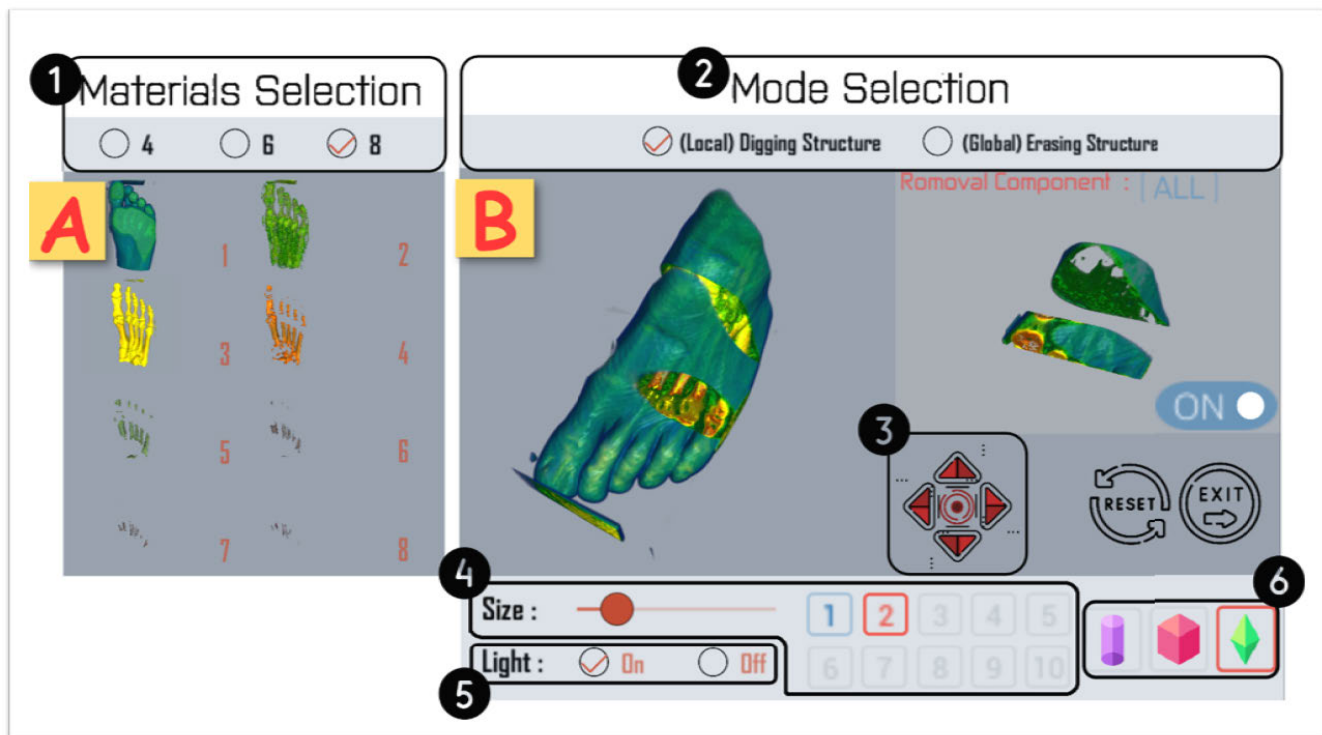


**FIGURE 1.** The user interface of the proposed system for non-expert users. (A) Navigation view gives non-expert users an overview of the materials structures of the dataset. The number of these major material structures is defined by a semi-automatic algorithm and data providers' decision. (B) Manipulation view is the main view for the users to interact with the dataset. More details of the interface will be described in Sec. IV.

also do not have explicit prior knowledge of the dataset. Thus, asking these users to spend hours learning how to manipulate visualization parameters to show the different structures of the dataset, such as adjusting complex transfer functions for direct volume rendering, is not practical. Although a few systems have been proposed in assisting non-expert users to explore 3D datasets [10], [11], these systems may need users to know what objects to look for and to have a certain level of understanding of the dataset or prior knowledge of the opacity function.

In conclusion, the challenges of non-expert users' exploration of a 3D dataset can be summarized as follows: (1) non-expert users usually only have inadequate understanding of the dataset, and (2) they only have limited time to familiarize themselves with a powerful but complex tool. Therefore, the goal of this work is to design a tool that will aid in the scenario. The objectives are as follows: (1) To show an overview of the dataset to non-expert users. (2) To create a tool with easy-to-learn interaction for data exploration that is adaptable to both mouse and touchscreen input devices. (3) To develop sufficient 3D contextual information to enhance the user's dataset exploration.

To achieve this goal, we mainly target medical datasets to propose a system that allows non-expert users to simply and interactively specify and remove the obstructing data to explore the internal structures of a 3D dataset. Because medical datasets usually consist of multiple materials, our

system first automatically analyzes the dataset to identify several major structures of the datasets by evaluating the shape similarity among isosurfaces. For example, major material structures could be the foot dataset's muscle or bond materials. Our system design also has the potential to be applied to non-medical datasets if the datasets also consist of obvious material structures. Each structure represents an isovalue range that contains isosurfaces without significant shape differences. Because of the above information, our system can properly remove a thick obstructing material structure specified by the users and reveal another material structure behind the obstructing one. In addition, we use a visibility-driven approach to predict what obstructing material in 3D space is specified by the users when the users can only point out the obstructing material on a 2D screen.

To remove the obstructing material structures, we propose two removal modes to preserve the proper context for data understanding and serve different users' purposes. The first is a local removal mode that allows users to dig out local obstructing materials through simple inputs. The progressive local digging interaction not only composes the mental context for users through the interactions but also creates spatial context around the digging region and can be considered like the real-life behavior of digging to find buried objects. Non-expert users can easily understand the interaction and processes of our system to learn a new 3D dataset. The second is a global removal approach that allows users to remove a

large region of the obstructing material structure efficiently. However, from simple user inputs, it is not easy to determine whether our system removes sufficient obstructing materials that match the users' expectations or already removed unseen data. Therefore, we develop a material segmentation approach to detect non-connected components to avoid removing unexplored parts of the data material. Should the users want to remove a larger region of data quickly, this design can better prevent removing unseen materials.

In the end, we develop a complete interface for the data providers, such as the museum engineers, to properly set up the data into our system and for non-experts users to quickly interact with a 3D dataset without a long training time. Fig. 1 is the interface for non-expert users. The non-expert users can both remove obstructing material structure to explore the dataset (Fig. 1(B)) and have an overview of the dataset (Fig. 1(A)) before they start to explore the data. In addition, we also allow non-expert users to remove obstructing structures at different parts of the dataset using different shape lenses (Fig. 1(6)) to better preserve the data context.

We used different datasets to demonstrate the capabilities of our system in Sec. V. We also did an evaluation with two studies. Study one discusses the usability of our tool and its' features using the System Usability Scale (SUS) and additional questions focusing on the tool digging modes. While the second study focuses on the comparison between our tool and Paraview. Moreover, in the second study, we also illustrate the versatility of our proposed system by applying it to non-medical volume datasets, thereby demonstrating its potential for application beyond the medical domain if the dataset also consists of multiple significant layer structures. In summary, the contributions of this study are threefold:

- A semi-automatic approach to segment 3D dataset into major layer structures to facilitate the setup of the dataset for exploration by non-expert users.
- An obstructing removal process that utilizes progressive digging interaction for non-expert users to intuitively identify and remove obstructing structures while maintaining good three-dimensional contextual awareness.
- A user-friendly interactive interface for both data providers and non-expert users, and a comprehensive evaluation of the proposed system.

## II. RELATED WORK

In this section, we review the basic information theory and some applications, and we also introduce previous works on occlusion management and deformation techniques.

### A. FEATURE EXTRACTION

Extracting volume features in the 3D space and using various techniques to emphasize the volume structure of interest can help users better understand volume data. The 3D region growth technique proposed by Huang and Ma [4] for volume visualization uses the partial or full region growth technique in its interactive dual domain interface. The work can shorten

the trial-and-error process of interactive data exploration. Recently, Xu et al. [12] proposed a survey to categorize four types of enhancement of characteristics (external, internal, structure, ideographic) in volume data. The transfer function is a commonly used technique that maps data volumes to colors and opacities to emphasize important structures in the volume-rendered images. Over the past few decades, researchers have developed new transfer function design algorithms to automatically extract important structures and emphasize them in the volume rendering images. Ma and Entezari [13] proposed an approach that uses feature visibility to measure opacity changes when designing 1D and 2D transfer functions. ImageVis3D [14] is a system that presents the visually segmenting results of a hierarchical classification in Intensity-Gradient 2D histograms to assist users in exploring volume data. Wang et al. [15] extended the visibility histograms proposed by Correa and Ma [16] to calculate feature visibility, which made the transfer function design more informative. Regarding feature analysis, the information theory proposed by Shannon [17] introduces the concepts of entropy and mutual information. Bruckner and Moller [18] can automatically detect representative isovales by using information-theoretic measures of similarity between isosurfaces. Wei et al. [19] are able to determine whether the pre-selected isosurfaces are representative by using information-theoretic to compare the level-set-based surfaces and true isosurfaces.

Most of the aforementioned approaches offer various methods for retrieving or displaying features that have significant scientific significance for users. For example, the approach proposed by Bruckner and Moller [18] requires the significant involvement of users to segment a dataset into significant layers. Based on their approach, we use a clustering algorithm to automatically group similar isosurfaces and reduce the workload for users when segmenting a dataset into multiple layers.

### B. OCCLUSION MANAGEMENT

Occlusion management is one of the major techniques to assist users in exploring 3D datasets. Elmqvist and Tsigas [20] proposed a taxonomy that classifies more than 50 methods into five design patterns: multiple viewports, virtual X-Ray, tour planner, volumetric probe, and projection distorter. Cui et al. [21] proposed a curved ray camera technique. Wu and Popescu [22] presented a multi-perspective focus and a context visualization framework, both of which are used to address data occlusion problems. Tominski et al. [23] presented functions of various lenses with the goal of selecting the proper lens for different data of interest based on the user's intent. Traoré et al. [10] proposed four requirements that most occlusion management methods cannot satisfy simultaneously and address the occlusion problem by gathering and scattering rays with lenses.

In addition, many previous works are inspired by illustrations or surgical ideas. Such as, Correa et al. [24] use

some operator functions as a surgical tool in the medical volumetric data exploration; Li et al. [25] use a metaphor of virtual retractor as a medical retractor for surgeries to perform cutting and splitting of a dataset. The approach considers physically-based technology to make the procedure looks natural. Stoppel and Bruckner [11] used a set of simple shapes to approximate complex structures with visualization results similar to the perspective illustration drawn by artists or illustrators. The previous approaches employed various metaphors inspired by real-life experiences to enhance scientists' intuitive understanding of the 3D context of the datasets during the obstruction removal process. In addition, Wu and Popescu [22] also survey and discuss the techniques to solve data occlusion. In their survey, they conclude one of the major concepts to solve the data occlusion problem is to enable local change. Inspired by the aforementioned survey, we develop the obstruction removal approach that simulates the digging behavior commonly observed in daily human activities to build users' 3D context while exploring the 3D dataset.

### C. INTERACTIVE VISUALIZATION

Originally, interactive visualization techniques were more PC-based, with input from devices such as keyboard and mouse. However, recently tablets have gained more popularity as an alternative to interactive systems, particularly among non-experts. For the small screen with touch control, a few approaches have been proposed. For example, Li and Shen [26] proposed an interactive system that combines a variety of interactive tasks on the touch screen. Furthermore, there have been studies for large touch screen devices, such as a multi-touch table system for orthopedic surgery planning and other applications [27], IsoCam, a novel indirect user interface for museum exhibitions [28]. Because of the widespread use of tablet devices and the above survey, our objective is to design an interactive process that allows users to intuitively point out the obstructing structures while being compatible with both PC and tablet platforms.

### III. ALGORITHM OVERVIEW

Our system design considers two types of users: non-expert users and data providers. Non-expert users are people who do not have strong prior knowledge about the data set and do not have a long time to interact with the data set. One example of the non-expert users is the visitors in the museum. Another type of users are the data providers, people that are going to setup the data into our system for non-expert users to explore. Data providers have much better knowledge about the dataset and scientific data visualization. One example is the scientists or engineers in the museum setting up the system. In order to serve these two types of users, we define the following four system design requirements:

- RQ1: Provide an overview and interface for data providers to setup the dataset for the non-expert users.

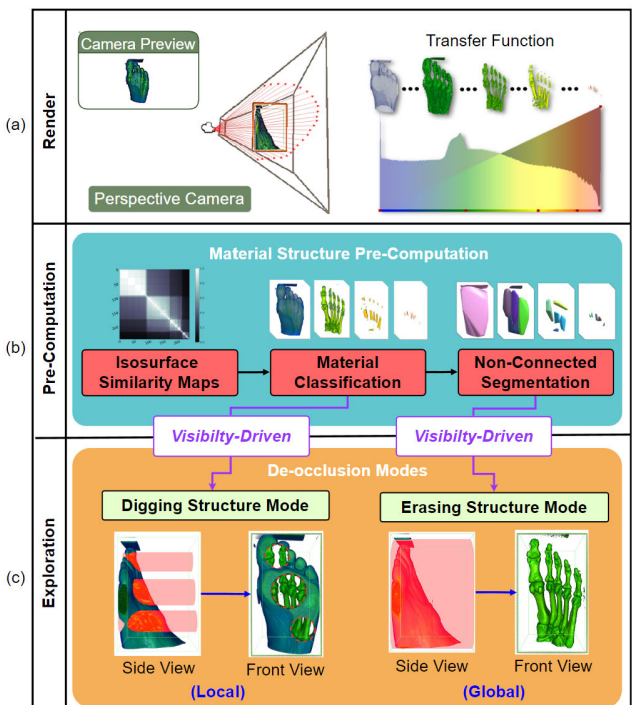


**FIGURE 2.** System overview. (a) The illustration of the configuration for the 3D data volume rendering in our system. The transfer function is set up by the data providers. The non-expert users do not have to touch the transfer function. (b) The preprocess to determine the number of major material structures and non-connected segmentation of each material structure. (c) The illustration of local digging structure mode and global erasing structure mode for non-expert users to remove obstructing materials.

- RQ2: Allow non-expert users to specify the obstructing structure on a 3D volume rendering image with a simple input on both touch and non-touch screens.
- RQ3: An obstruction structure removal process that assists non-expert users to easily understand the removal and the revealed structures.
- RQ4: Provide a comprehensive and intuitive interface for non-expert users to smoothly explore each structure of the dataset.

In the following, we use a foot dataset to illustrate our system (Fig. 2) and briefly describe how it tackles the challenges and satisfies our requirements. From top to bottom, our algorithm is divided into three stages: volume rendering, volume pre-computation, and volume exploration.

When the data providers, such as the high school teacher or museum scientists, load the data into our system, our system will evaluate the isosurface similarity to segment the 3D data into multiple material structures and compute non-connected components of each material structure before the non-expert users start to explore the data (Fig. 2(b)). The segmentation process is automatically done by our system. The data providers only have to select the desired number of layer structures and assign the opacity and color to the different material structures. Figure 3 shows the interface for data providers. At the top of the left-hand side of the interface,

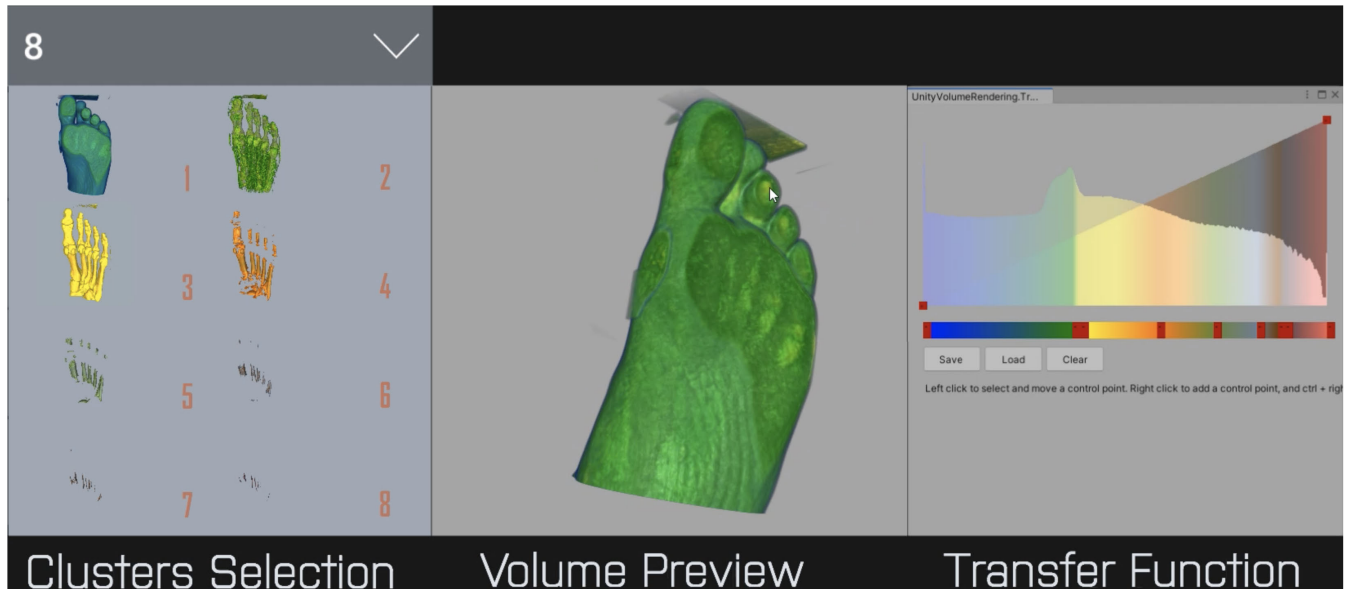


**FIGURE 3.** Data provider interface. The interface is divided into three views. The data provider can select the number of layer structures and observe each layer in the cluster selection view, setup the color and opacity of each layer structure in the transfer function view, and preview and interact with the data in the volume preview view.

the data provider can select a desired number of layers for non-expert users through the drop-down menu. Then, the individual layer with the selected number of layers is displayed on the main view of the left-hand side of the interface. Once the number of layers has been determined, the data provider can adjust the opacity and color for each layer via the panel on the right-hand side. Additionally, the data provider can have a preview and interact with the dataset using the current settings in the view in the middle view. In addition, our system also shows the individual layer structures to the non-expert users to help them acquire the basic structural awareness of the volume data before beginning to interact with it, which fulfills requirement RQ1 and the corresponding challenge. The details will be discussed in Sec. III-A.

Fig. 2(a) illustrates the volume visualization process. Our system uses direct volume rendering to render the 3D data volume inside the predefined green bounding box  $S_{box}$ . Each pixel emitted from the camera position is divided into  $n$  sample points. The data value corresponding to the sampling point falling in the  $S_{box}$  is mapped to the material's color and opacity defined by the data provider. However, non-expert users do not need to know this visualization process and only have to pay attention to the volume data displayed on the screen.

Figure 2(c) presents the procedure for removing obstructing structures. We adopt a visibility-based approach for identifying the obstructing structure along the depth direction indicated by the user. Because of the visibility-based approach, the system allows users to use a simple clicking or pressing on the obstructing structure they see to specify the obstructing structure, which fulfills requirement RQ2 and tackles the corresponding challenge. In order to develop 3D contextual information for non-expert users, we provide a

digging structure mode that enables users to locally explore regions of interest. This interaction allows users to progressively remove obstructing structures, and it is similar to the digging behavior in the real world. Non-expert users can easily understand the interaction and develop 3D contextual information, which fulfills requirement RQ3 and tackles the corresponding challenge. After the users think a material structure has been well explored, an erasing structure mode is provided to remove and explore the entire connected structure globally. The details will be discussed in Sec. III-C.

#### A. MATERIAL STRUCTURE PRE-COMPUTATION

In many classic 3D visualization tools, users need to manually adjust complex transfer functions to explore the structures of 3D dataset. Our work's focus is to facilitate 3D data exploration for non-expert users, so it is not practical to ask non-expert users to learn how to adjust the complex transfer function. Therefore, the primary task in this pre-computation stage is to compute material structures with significantly different shapes and segment the 3D dataset. For example, this pre-computation method can segment a foot dataset into the muscle, bone, and two other internal bone structures in Fig. 2. This information allows data providers to conveniently assign opacity and color to the extracted major material structures for volume visualization and provide non-expert users an overview of the dataset before starting the exploration. In addition, this information is also utilized in the obstructing object selection step to simplify manipulations for non-expert users.

In order to divide a dataset by a few major material structures, we are inspired by previous research by Bruckner [18] and Wei et al. [19]. Both works integrate different techniques based on information theory to identify the most

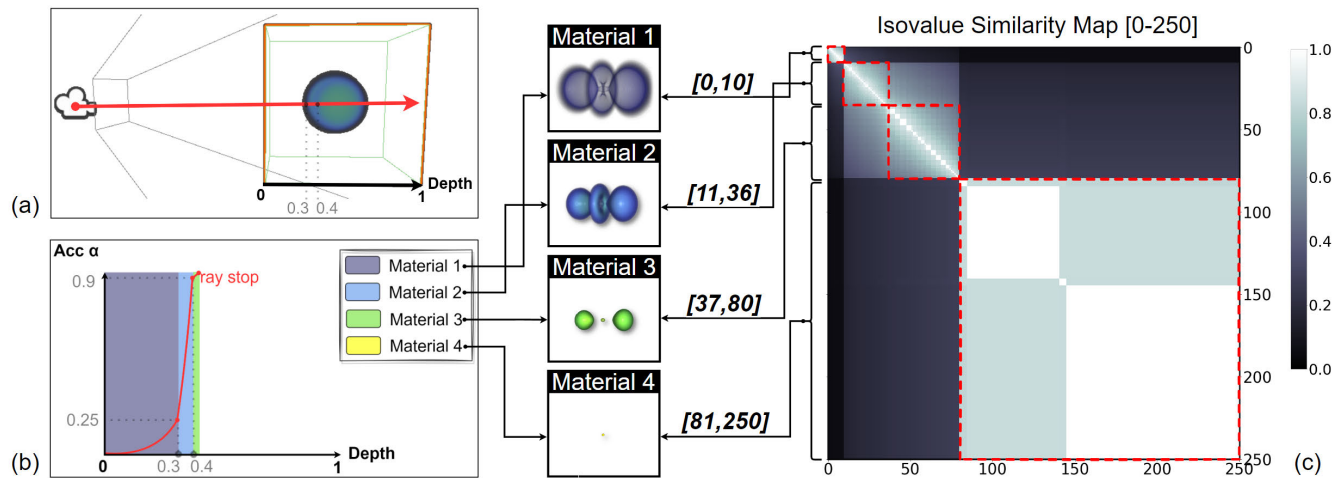


**FIGURE 4.** (a) Illustration of a single ray that is cast in the direct volume rendering algorithm and the ray is selected by the non-expert user when the user sees the obstructing material on the corresponding pixel. (b) The visibility-driven approach to detect user-selected obstruction. This figure represents the cumulative opacity function of the red arrow ray in (a). (c) The isosurface similarity clustering-based approach to identify main material structures. The heatmap shows the similarities of all isosurfaces pairs and the clustering result for the Hydrogen Atom dataset when the number of the cluster is set to four. The images in the middle are the material structures of the four isovalue clusters.

representative material structures. We utilize the concept of isosurface similarity to automatically identify the most representative material structures of a dataset. We first measure isosurface similarity of all pairs of possible isovalue's isosurfaces by calculating the shortest distance from each vertex in space between isosurfaces. Similarity value ranges from 0 to 1 according to their similarities range, with 0 meaning that the two isosurfaces have no similarities and 1 meaning that the two isosurfaces are the same. After the computation, we can virtually create an isosurface similarity map showing Fig. 4(c). Note that the isosurface similarity map is only shown to the data providers to set the dataset into our system. The isosurface similarity map is not shown to the non-expert users and they do not need the information from this map to explore the 3D dataset.

In order to allow data providers to more quickly and flexibly identify isovalue ranges for major material structures, and set up the dataset for non-expert users, we use a hierarchical clustering algorithm [29] to cluster the isovalue into  $N$  isovalue ranges. Data providers can give the desired number of material structures,  $N$ . The hierarchical clustering algorithm will evaluate the isosurface similarity map. If the isovalue's isosurface shapes are similar, the isovalue should be clustered into the same cluster. As Fig. 4(c) shows, the clustering result will be shown to the data providers. The data providers can iteratively try different  $N$  values to find the desired number of major material structures. After data providers determine  $N$ , because the dataset is divided into a few material structures, they can easily assign the color and opacity for each material structure.

Fig. 4(c) illustrates this process to calculate material structures from an atom dataset. The isosurface similarity map shows the similarity values among all pairs of isosurfaces. The x- and y- axes are isovalue, and the brighter blocks along

the diagonal represent isosurfaces of isovalue with similar geometric structures. Note that this isosurface similarity map is only shown to the data providers to select major material structures. The data provider can select the desired number of material structures,  $N$ . Fig. 4(c) shows the hierarchical clustering result when the data provider set  $N$  to 4. The red rectangles indicate the 4 clusters' isovalue ranges. According to the four isovalue ranges, the whole atom dataset is subdivided into four main material structures with significantly different shapes, which is shown in the middle of Fig. 4. After the data provider sets the color and opacity the four material structures, the dataset is successfully set up in our system, and the non-expert users can start interacting with the dataset.

## B. INTUITIVE OBSTRUCTING STRUCTURE SELECTION

According to requirement RQ2, our system design should allow users to intuitively select the obstruction with simple inputs. Therefore, we follow the WYSIWYG (What You See Is What You Get) principle to design our obstruction selection function. Users can just click or press on the obstruction when they want to select an obstruction and explore the material behind it. However, when a 3D dataset is visualized by direct volume rendering, the material could be semi-transparent, and the color of a pixel could be composed of multiple different materials. When the non-expert users click on the screen, they only select a pixel ray instead of selecting a point in the 3D space. Therefore, we cannot directly know which material they point to. In order to determine which obstructive material non-expert users want to select along the pixel ray, we utilize the visibility-oriented picking technique. The idea of the visibility-oriented picking technique is to analyze which material contributes the most opacity to the pixel color to predict which material the users want to select along the pixel ray. A classic visibility-oriented picking

technique [30] has to compute the first and second derivative of the ray's accumulated opacity to determine the maximum opacity value change of material to determine the selected material. In order to efficiently calculate the selected material, we can use the pre-computed material structures in Sec. III-A. We calculate each material structure's ray-accumulated opacity, and visibility (*alpha*), to determine the most visible material. Fig. 4(a) and Fig. 4(b) show the obstruction selection on the hydrogen atom dataset. Fig. 4(b) illustrates the accumulated opacity value of the pixel ray of the selected pixel (red arrow) in Fig. 4(a). The colors in Fig. 4(b) represent different material structures along the selected pixel ray and the y-axis represents accumulated opacity from the camera view. In the example in Fig. 4, cluster 2 has the maximum visibility contribution because the accumulated opacity within cluster 2 is larger than that of other clusters. Therefore, when non-expert users click on this pixel, we predict that the users select material 2 as the obstructing structure.

### C. OCCLUSION REMOVAL

Our system provides two obstruction removal modes, local digging structure mode, and global erasing structure mode. The local digging structure mode removes the obstruction locally and keeps the context around the local region. The global erasing structure mode allows users to remove a whole material structure quickly. This section is going to introduce the details of these two modes.

#### 1) LOCAL DIGGING STRUCTURE MODE

The main goal of this digging structure mode is to simulate the behavior when a person digs out material along the view depth direction. The person keeps digging out the obstructing material until the person touches and reveals another material structure. We use Fig. 5 to illustrate the local digging structure mode. Fig. 5(a) is a sphere with a gold surface. Fig. 5(b) is a hand-drawing perspective view to show the structures of the dataset. The big gold sphere contains three smaller spheres with different sizes. If the user clicks at the red dot on Fig. 5(a), it means that the user would like to remove what the user sees at the red dot and explore the data behind it. In this case, the users would like to remove the gold material to explore the data behind it. Fig. 5(c) (front side view) and Fig. 5(d) (back side view) are the result when the non-expert users select the gold material as the obstructing material structure to dig out in Fig. 5(a). Because the upper part and bottom removed parts in Fig. 5(c) are all gold materials along the view depth direction, they are fully removed. The gold material in the middle part in Fig. 5(c) is removed until another material structure (orange material) is revealed. In addition, the goal material behind the orange material (Fig. 5(d)) is still preserved for the users' further exploration.

To implement the local digging structure mode, we present a local lens placement to dig out the selected obstruction from Sec. III-B in the lens region. When users click on the screen, the clicking point will be the center of the lens. Our system

then calculates each pixel ray in the lens region independently to identify the obstructive material by the algorithm introduced in Sec. III-B. The system will then dig out all samples from the camera to the selected obstructive material. The removal process means the samples of these materials will be ignored in the rendering pipeline. Fig. 5(f) shows the circle focus lens used in this example. The pixel rays inside the region compose a red cylinder region. Our system will process all the pixel rays inside this cylinder region to remove the obstruction.

We also use ray 1 and ray 2 in Fig. 5(f) and (g) to illustrate the implementation procedure of our local digging structure mode removal algorithm in detail. Ray 1 and ray 2 are two rays inside the lens. The orange point represents the boundary of the selected obstructive material close to the camera, and the green point is the boundary of the selected obstructive material on the other side. From ray 1, it can be seen that the visible structure of an entirely golden block region will be removed, while from ray 2, it can be seen that the orange structure and the gold material behind the orange structure will remain because these materials are behind the green point.

Furthermore, to keep more context for users, our system allows users to dig out multiple local regions, or multiple obstructive materials along the view depth direction. Fig. 5(e) shows the results after the user clicks once at the right hollow's center and twice at the blue arrow. Because the user only clicks once at the right hollow, only one material structure (gold surface) is dug out. The user clicks twice at the blue arrow region, so two materials (gold and orange) are dug out, and the internal dark orange material is revealed. In addition, our system does not only provide one lens shape for non-expert users. We define three different shapes of lenses, circle, retractor, and cuboid, for non-expert users to freely select the proper lens shape to remove the obstructing material when exploring the different portions of the dataset. Fig. 11 illustrates the three shapes of lenses and the use of applying them to different parts of the head datasets.

#### 2) GLOBAL ERASING STRUCTURE MODE

The non-expert users sometimes may want to quickly remove a whole selected obstructing material structure, such as the whole gold material in Fig. 5, instead of digging out a lot of "holes" to remove it. In addition, after the users dig out multiple "holes" and get a sense of a material structure, they may want a more efficient function to remove the whole obstructing material structure. Therefore, our system provides a function called global erasing structure mode to allow users to remove a whole material structure with one simple click. However, by the material structure pre-computation introduced in Sec. III-A, one material structure consists of the isosurfaces of an isovalue range. Therefore, the material structure could consist of multiple non-connected pieces, which could spread over different locations in the data volume space. If we directly remove all the pieces of the selected material structure, we may remove some pieces that the users

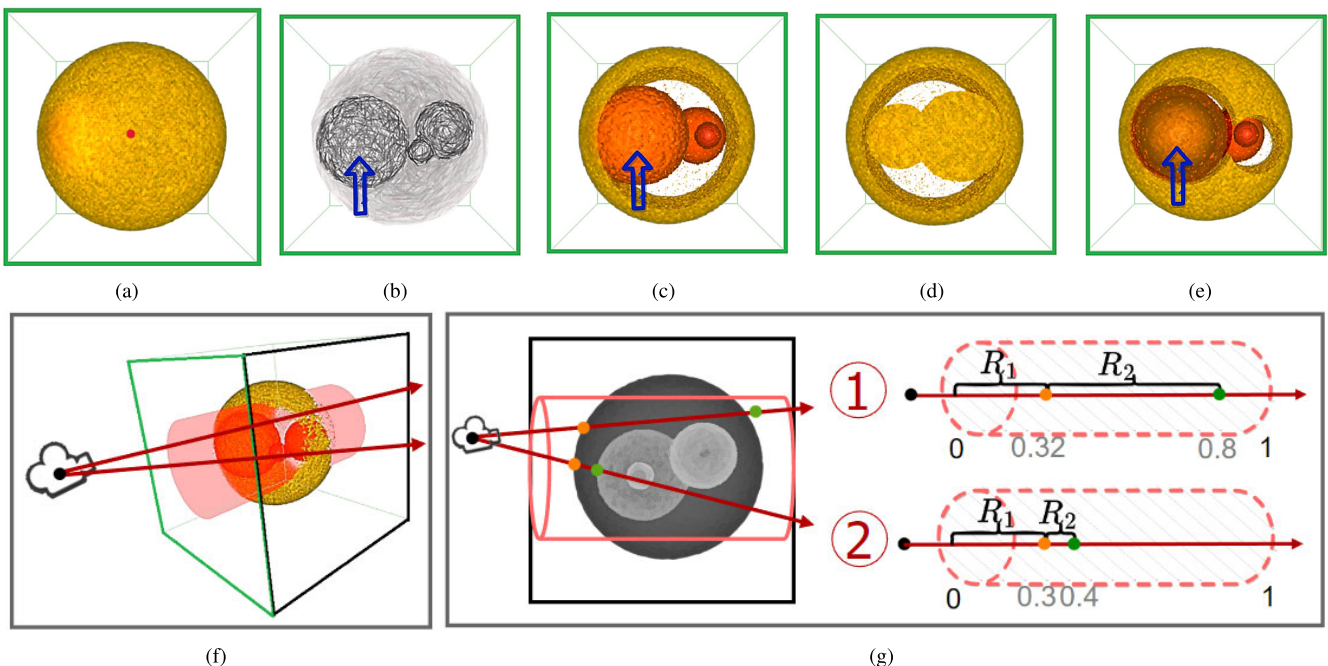


**FIGURE 5.** Illustration of the local digging structure mode. (a) shows the dataset before the removal operation. (b) shows a hand-drawn perspective view of the dataset. (c) shows the result when the user clicks once at the red dot in (a). (d) is the opposite side of (c). (e) shows the result when the user clicks twice at the blue arrow and once at the center of the right hollow. (f) shows the side view of the lens of (a) when the user clicks on the red dot in (a). (g) shows two rays that pass different portions of the dataset to show how the digging structure mode works.

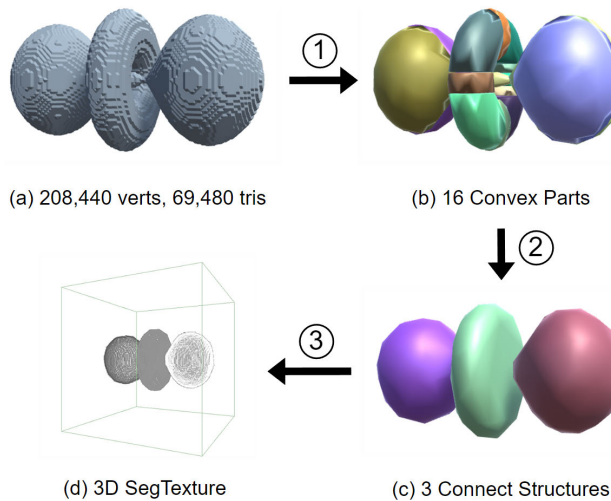


**FIGURE 6.** The overview of the segmentation algorithm. (1) Decomposition of the material structure shown in (a) to calculate for the convex parts. (2) The mesh collision detection combines convex parts into three non-connected components. (3) Transfer the segmentation result into the texture memory for the non-expert user interaction stage to use.

never see, and the user may never know the pieces that exist in the dataset. In addition, this way can keep more context for the users. Therefore, the global erasing structure mode should only remove the selected piece, instead of removing all non-connected pieces of the select obstructing material structure.

When a material structure is selected as an obstruction, we have divided the material structure into connected components. The segmentation algorithm is illustrated in Fig. 6 and we use the material structure 2 of the atom data in Fig. 4 as an example. The material structure of the hydrogen atom is composed of 208,440 vertices and 69,480 triangular faces, as shown in Fig. 6(a), we use the segmentation algorithm [31] proposed by Mamou and Ghorbel to merge any triangle meshes as convex solutions. The algorithm approximates 16 parts of convex decomposition structures in this situation, as shown in Fig. 6(b). Then, the mesh collision detection is executed. The meshes that collide with each other are considered as connected structures and combined into the same piece. Fig. 6(c) show 3 connected components after the convex parts are merged. Finally, we save the segmentation structure in the 3D texture to be used in the rendering stage, as shown in Fig. 6(d).

Therefore, if the non-expert users observe and consider the material structure 2 in Fig. 6(c) as an obstructing structure and click on the purple piece, our system will only remove the purple piece instead of the whole material structure 2. Our system allows the user to control the animated transition to make the piece invisible from the clicking point to the whole piece.

#### IV. INTERACTIVE EXPLORATION SYSTEM

This section will introduce each view in our system interface (Fig. 1) and their functions in detail.

- **Navigation View** (Fig. 1(A)). The navigation view is an overview for non-expert users to browse the material structures of the dataset. As we mentioned in Sec. III-A, the data providers and the pre-computation algorithm determine the number of material structures. In addition, we also allow the data provider to set up a different number of materials for the non-expert users to select when exploring the dataset (Fig. 1(1)). By browsing this view, users can develop a rough mental map of the dataset to start the data exploration. Therefore, users can more easily know whether the target structure has been revealed and observe the 3D context around the structure.

- **Manipulation View** (Fig. 1(B)). This view consists of two display areas and multiple control panels. The display area on the left-hand side is the main display. The main display shows the volume rendering result, and the non-expert users can specify the obstructing structure to remove on this display. The display area on the right-hand side shows the obstructing structure that is just removed from the main display. This display provides more context to users to understand the removing and remaining parts of the dataset.

**Mode Selector:** (Fig. 1(2)) The control panel for users to select local digging structure mode or global erasing structure mode to remove the obstructing structure.

**Orientation Controller:** (Fig. 1(3)) The non-expert users can usually rotate the data by dragging the data on the display area. This controller allows users to rotate the data by 90 degrees along a single axis.

**Lens Shape Selector:** (Fig. 1(6)) We provide three distinct lens shapes, round, square, and retractor, allowing users to select different lens shapes for a particular portion of the volume. Users can select different lens shapes by this selector.

**Lens Size Slider:** (Fig. 1(4)) When the system applies a lens to remove the obstructing structure. The user can control the lens size by this slider.

**Light Switch:** (Fig. 1(5)) Our lighting model consists of diffuse and glossy illumination. The users can enable or disable the illumination effect to render the dataset.

## V. CASE STUDIES

We explore the different applications of our tool for non-expert users in this section. The first case uses the demonstration of the kidneys' dataset, showing how non-expert users can easily explore the dataset by using our system. The second case uses an atom dataset to show how our system can better help non-expert users preserve the context of the dataset when they use the tool's mode to remove structures compared to another scientific 3D visualization tool like Paraview. The last case uses a human head dataset to demonstrate how different lens shapes can better remove obstructing structures from a different portion of the dataset. The study not only uses medical image volume datasets but also incorporates non-medical image volume datasets to

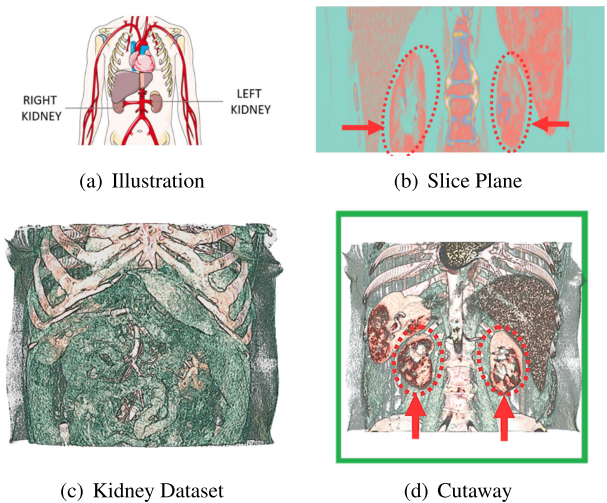


**FIGURE 7.** (a) Illustration of the arterial circulation from Servier Medical Art. (c) Kidney visualization using our system before the obstructing material structure removal. (b) is the visualization to show the kidneys and the tumor by the classic slice plane technique. (d) is the visualization to show the kidneys and the tumor by the classic cutaway technique.

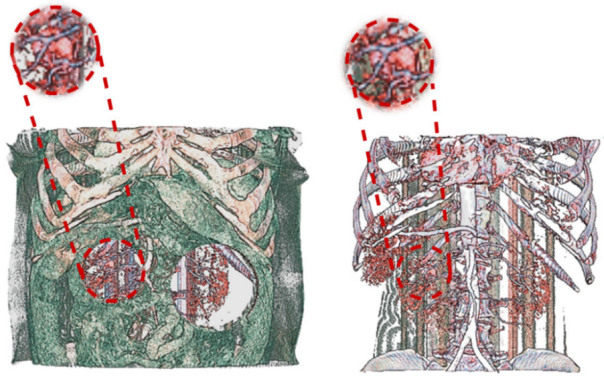
demonstrate the versatility of our system when using diverse dataset and in other cases where the dataset consists of multiple significant layer structures.

### A. USE CASE 1: KIDNEY DATASET

Kidneys are paired bean-shaped organs placed on both sides of the posterior lumbar spine that belong to the urinary system of the basic organ system of the human body [32], as shown in Fig. 7(a). In this case, we assume the non-expert users already know that the main purpose of interacting with this dataset is to explore and observe the tumor on the kidney. Therefore, their goal is to first locate the kidneys and then compare the difference between kidneys to find the tumor. In the beginning, the dataset is rendered as Fig. 7(c) for users to start the exploration. The user first clicks around to dig out the obstructing materials around the kidneys' location to locate the kidneys. Through this interactive digging and revealing structures process, the user can have a better context on the relative position of the kidneys. An intermediate result will be that the user discovers the location of kidneys is shown in Fig. 8(a). After locating the kidneys and knowing what material (the green one) occlude the kidneys, the user uses the global erasing structure mode to erase the whole green material to more easily observe and compare the two kidneys and observe the tumor on the right kidney. The result is shown in 8(b). Because of our material structure pre-computation, different material structures of the dataset are well separated at the data preparation stage and used to configure our system by the data provider. Therefore, non-expert users can reveal and observe the kidneys with clear internal blood vessels and tumor boundaries by just a few simple clicking.

### B. USE CASE 2: ATOM DATASET

The physicist Rutherford initially proposed a model of atomic structure in 1911 [33]. As shown in Fig. 9(a), the nucleus



(a) Local Digging Structure Mode (b) Global Erasing Structure Mode

**FIGURE 8.** Exploration for the tumor on the kidney by our system. (a) is the result from the local digging structure mode (b) is the result from the global erasing structure mode. The zoom-in view is the tumor on the kidney. The internal blood vessels and the tumor can be observed clearly by both modes.

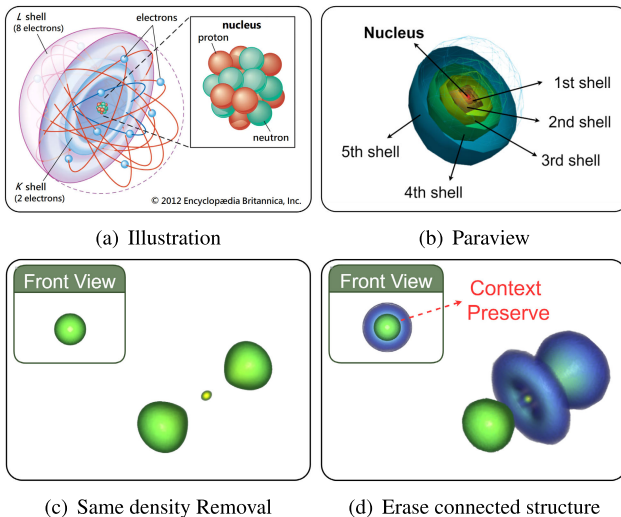


**FIGURE 9.** (a) Illustration of a shell atomic model (Copyright ©2012 Encyclopaedia Britannica, Inc. All rights reserved.) (b) Images constructed using the 3D Paraview visualization tool. In (c) and (d), both users click on the left part of the blue material structure to reveal the internal green material structure using the global erasing structure mode. (c) uses the global erasing structure mode without non-connected component segmentation. (d) uses the global erasing structure mode with non-connected component segmentation.

comprises of protons, neutrons, and electrons that can be found in a shell at a particular distance from the nucleus. Each shell layer looks like an onion from the outside to the interior. The primary goal of this use case is to show how non-expert users can understand the illustration structure of the atom shown in Fig. 9(a). We also compare the usability of our system with Paraview [34], a popular scientific data visualization software, for non-expert users, and the difference between using the non-connected component segmentation introduced in Sec. III-C2 and without it.

In order to show the multi-shell structure on Paraview, we manipulate Paraview to produce the visualization in

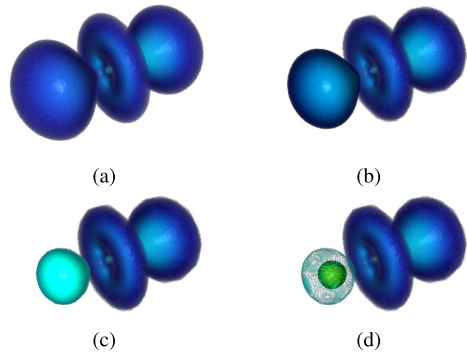


**FIGURE 10.** Illustration of steps to interactively explore the left shell group. (a) is the view without any obstructing structure removal. (b) to (d) are shown after the user clicks on the left shell group in (a) to (c), respectively.

Fig. 9(b). To produce the image in Fig. 9(b), we have to manipulate Paraview to extract the isosurfaces of multiple shells, execute the plane cutting to show half of the shells, and change the opacity of the cutting range. By the above complex steps, the center of the atomic cross section and the surface of the outer shell can finally be observed. However, going through the above steps and producing the image is not easy for a non-expert user.

In contrast, our system allows users to interactively remove the obstructing shell and reveal the internal shells by simply clicking on the obstructing shell. The designed manipulation of our system is intuitive and easy to use by non-expert users, and this interactive data exploration can also develop the mental context for users to learn the multiple shell structure of the atom. Figure 10 shows the steps to interactively explore the left shell group. By every click on the left shell group, one obstructing shell is removed, and one more internal shell is revealed.

In addition, we develop the non-connected component segmentation technique in Sec. III-C2 to only remove a connected material structure when users click on the obstructing material. This technique can preserve a better context for users to observe and understand the dataset. Fig. 10(d) is the obstruction removal result with the non-connected component segmentation when users click on the left shell group to remove an outer blue shell and reveal the internal green shell. Fig. 10(c) is the obstruction removal result without the non-connected component segmentation when users click on the same obstructing structure. When users click on the left shell group, the user could mentally divide the dataset into left, middle, and right parts, and the user only focuses on the left shell group. Only removing the blue material on the left shell group (Fig. 10(d)) better fits the user's mental assumption and preserves more context for the user than Fig. 10(c).

### C. USE CASE 3: HUMAN CT DATASET

Our system provides cylinder, cuboid, and diamond lens shapes for users to dig out obstructing structures. In this

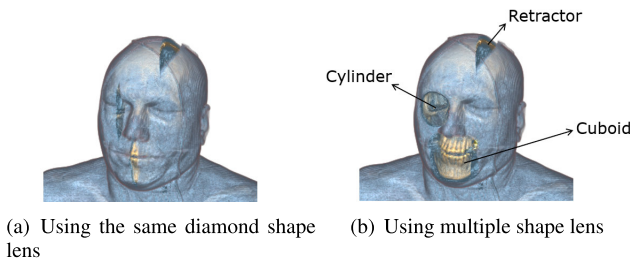


**FIGURE 11.** The comparison of using single shape lens only and multiple shape lenses on different parts of the CT dataset.

section, we use the visible human CT head volume dataset to demonstrate that different regions of the dataset could need different shapes of lenses to be explored more effectively. Therefore, allowing users to freely select different lens shapes to dig out obstructing material can benefit data exploration. The dataset is a native UVF format dataset provided by the ImageVis3D program developed by the NIH/NIGMS Center for Integrative Biomedical Computing [35]. The dimension is 512 X 512 X 512. In Fig. 11(a), we dig out the muscle at the mouth, head, and eye regions with diamond shape lens only. We can observe that the diamond shape lens fits the head well. However, the diamond shape lens can only dig out a long and slim hole around the eye region and cannot keep the proper context to observe the data around the eye region. In Fig. 11(b), we use the diamond shape lens to dig out the material at the head region, the cylinder shape lens to dig out the obstructing material at the eye region, and the cuboid shape lens to dig out the obstructing material at the mouth region. Using different shape lenses at different regions, we can dig out a region and keep the proper context for users to easily observe and understand the dataset.

## VI. EVALUATION

To evaluate the tool in different aspects, we conducted two studies. In study 1, we evaluate the system usability using the System Usability Scale (SUS) and additional questions we create to evaluate the (Local) Digging Structure and (Global) Erasing Structure mode from the tool. Study 2 compares our tool capabilities and features with Paraview, a commonly used tool in scientific 3D data exploration.

### A. STUDY 1: SYSTEM USABILITY

System usability is how effectively the user can utilize the tool. For this study, we use System Usability Scale (SUS). In addition, four additional questions were added to assess the usability of the tool's two modes and participants' preferences. To provide qualitative usability value, semi-structured interviews were conducted with some participants.

#### 1) SYSTEM USABILITY SCALE (SUS) MEASUREMENT

The System Usability Scale (SUS) was first introduced by John Brooke in 1986 [36]. The SUS was selected for this study because it is a popular and reliable method used

as a quick way to measure the usability of a tool [37]. To increase the accessibility of the questionnaire, the participant were given the Chinese translation of the SUS. Yuhui Wang et al. [38] had provided a Chinese translation of the SUS, which had been tested for good reliability.

SUS consists of a 10-item questionnaire that measures the user's subjective assessment of the usability of the system. There are ten questions in the SUS scored on a five-point Likert scale [39] ranging from "strongly agree" to "strongly disagree". In SUS, odd-numbered questions are phrased positively, and even-numbered questions are phrased negatively [40]. To calculate the SUS score, odd-numbered item scores are calculated as the scale position minus 1, while even-numbered item scores are calculated as 5 minus the scale position. Each item score is then multiplied by 2.5 to produce a score that ranges from 0 to 10 in increments of 2.5. With 0 indicating poor usability and 10 indicating excellent usability. Note that even-numbered questions are reversed before averaging with odd-numbered questions, resulting in a higher SUS score indicating better usability regardless of question phrasing. Then, to calculate the final score, each item's score is then summed up to create a score ranging from 0-100.

### 2) DATA COLLECTION PROCEDURE

Twenty-five participants (female n=13, 52%) participated in Study 1. Most of our participants are between the age of 18-25 (n=13, 52%) followed by nine (36%) participants between the age of 26-35 and the rest above the age of 35. Ten (40%) participants are still students, with seven of them pursuing master's degrees. While eight (32%) participants with bachelor's degrees and five (20%) participants with master's degrees. This study's participants also come from different fields of study/work. The highest number of participants have an engineering background or are currently working in engineering (n = 18, 72%). While others come from various fields, such as English (n=2, 8%), business and finance (n=2, 8%), education (n=1, 4%), Chinese as a second language (n=1, 4%), and human development and family studies(n=1, 4%).

First, participants are shortly briefed about the test session and information about the questionnaire and procedure. Participants were then given time to read and sign the informed consent form as well as fill out the demographic questions.

Participants are then asked to watch a 2-minute and 20-second video introducing the tool. The video introduces the participants to the tool's goal of removing occlusion when viewing 3D datasets. It also demonstrated the tool's main menu for selecting which dataset to use and provided a brief overview of the tool's features, like (Local) Digging Structure mode and (Global) Erasing Structure mode, and various buttons of the tool. After that, the participants were shown the tool and given time to play around with the tool. In this stage, participants are allowed to ask the researcher to clarify questions they might have. When they feel like they

**TABLE 1.** System Usability Scale (SUS) result of our tool. After the score transformation, all higher SUS item scores will indicate better usability.

Questions	Score					Mean	SD
	0	2.5	5	7.5	10		
1. I think that I would like to use this system frequently	2	3	7	8	5	6.1	2.98
2. I (don't) found the system unnecessarily complex	1	0	4	6	14	8.2	2.55
3. I thought the system was easy to use	1	0	2	9	13	8.3	2.36
4. I (don't) think that I would need the support of a technical person to be able to use this system	1	5	5	10	4	6.1	2.80
5. I found the various functions in this system were well integrated	0	1	6	13	5	7.2	1.95
6. I (don't) think that there was too much inconsistency in this system	0	0	5	9	11	8.1	1.95
7. I would imagine that most people would learn to use this system very quickly	0	0	3	7	15	8.7	1.79
8. I (don't) found the system very awkward to use	0	1	4	5	15	8.4	2.27
9. I felt very confident using the system	0	0	0	13	12	8.7	1.27
10. I (don't) need to learn a lot of things before I could get going with this system	2	3	4	6	10	6.9	3.33

**TABLE 2.** Additional questions created specifically to evaluate the (Local) Digging Structure and (Global) Erasing Structure mode from the tool.

Additional questions	Mean	SD
1. I think the (Local) Digging Structure mode is easy to use.	4.04	1.17
2. I think the (Global) Erasing Structure mode is easy to use.	4.12	1.12
3. I prefer using the (Local) Digging Structure mode rather than the (Global) Erasing Structure mode	3.2	1.01
4. I have a clear understanding of which part of the 3D model is removed when I use the tool.	4.12	1.09

have explored the tool enough, participants are then asked to fill in the SUS questionnaire, our additional questions for the “digging” feature. Some participants that already agreed beforehand are asked for semi-structured interviews to understand their answers better.

### 3) RESULTS

Table 1 summarized all the feedback collected from twenty-five participants toward ten SUS statements by showing the frequency of each score in each question. As the explanation in Sec. VI-A1, the items’ score transformation will make any higher SUS item score means higher usability. The highest score average was on question 9 “I felt very confident using the system” with an average score of 8.7 (SD=1.27) and question 7 “I would imagine that most people would learn to use this system very quickly” also with an average score of 8.7 (SD=1.79). This is followed by question 8 “I (don’t) think the system is awkward to use” which had an average score of 8.4 (SD=2.26) and question 3 “I thought the system was easy to use” with an average score of 8.3 (SD=2.36).

The reason why the majority of people feel confident using our tool and believe that others can learn this system quickly may be attributed to the simplicity of the tool interaction and the comprehensibility of the progressive removal process, which most people perceive positively. Participants’ explanations in the post-interview also help corroborate these potential reasons. For example, when asked what participants think about our tool, one of them states that “*In my opinion the tool*

*is easier to use than I expected*”. Another user said that “*the tool is simple enough that children can probably use it*”.

Previous studies have shown that if a tool is considered good or has high usability, it has to have a final score of more than or equal to 68 [38], [41]. Our tool has an average SUS score of 76.7 which is higher than 68, with only four users’ (16%) scores below 68, which shows that our tool can be considered good or has high usability.

In addition to the System Usability Scale (SUS), we included Likert-scale questions, ranging from 1 (strongly disagree) to 5 (strongly agree) in order to evaluate the two modes in our tool, (Local) Digging Structure and (Global) Erasing Structure. The first two questions specifically aimed to assess the ease of use of each mode individually. The third question was created to determine which mode participants preferred using. Lastly, the fourth question was added to measure the extent to which participants agreed that they understood the actions they were performing in the tool using the modes, rather than clicking the button randomly.

Table 2 shows the results of the additional questions. Participants found the (Global) Erasing Structure mode easier to use than the (Local) Digging Structure mode, with scores of 4.12 (SD=1.12) and 4.04 (SD=1.17) out of 5, respectively. Participants did not strongly prefer one mode over the other, with a score of 3.2 out of 5 (SD=1.01) for preferring the (Local) Digging Structure mode. Participants were confident in their understanding of how to use both modes, with a score of 4.12 (SD=1.09) out of 5.

### B. STUDY 2: COMPARISON WITH PARAVIEW

One of our goals is to create a tool with easy-to-learn interaction for data exploration while developing sufficient 3D contextual information to enhance the user’s dataset exploration. A closer study is needed to evaluate the proposed tool.

For this study, participants were tasked to work on an object-finding task we named “Find-the-Lobster” using both our tool and the Paraview tool. In “Find-the-Lobster”, participants are shown a 3D object of a teapot. The participants are then told that there is a lobster object inside the teapot and the participants need to find a way to show the lobster.

When trying to complete the “Find-the-Lobster” task using either our tool or Paraview, participants are encouraged

to try to complete it by themselves. However, since most of them have very limited knowledge of scientific visualization, it is understandable that they might get confused about what to do. Thus, participants are allowed to ask for hints or redirection if they have strayed too far from the goal. When the participant asked for hints, the interviewer will provide some hints (the time taken to explain the hint won't be counted in the completion time) before letting the participant try again. If the participant ended up giving up, we will then provide them with the answers to the task.

To complete this task with our tool, the participants need to use either the digging feature or the global erase feature that we have. On the other hand, to complete the task with the Paraview tool, we provide them with the transfer function tool, one common way to visualize the internal structure of a 3D dataset. The participants are required to tune the transfer function until the lobster is visible. After they finished the task, participants did semi-structured interviews to help researchers further understand their criticisms and comparison of both tools.

### 1) PARAVIEW

Paraview is an open-source scientific data visualization and volume exploration tool [34], [42]. It was first developed in 2000 by Sandia National Laboratories and Kitware, Inc., and has since become popular for scientific data explorations [34]. One of the key features of Paraview is the ability to perform advanced visualization such as volume rendering. When visualizing 3D datasets using the direct volume rendering technique, Paraview users can tune the transfer function by assigning opacity and color to different data values to show the internal structures of datasets.

### 2) DATA COLLECTION PROCEDURE

Seven participants (female n=5, 71%) were asked to join this evaluation. Out of seven participants, five of them (71%) are not in Computer Science (CS) background or working in the computer science field. The involvement of participants with a CS background might be beneficial in evaluating this new tool because they may be more familiar with learning a new tool. However, we also believe that individuals with a non-CS background can also provide important insight, especially since our target audience may not have a technical background. Therefore, we think it is important to provide the demographic of the study's participants which are shown in table 3.

Participants are first briefed about the survey form and the study's procedure. The participants then start reading and signing the informed consent form and then answered demographic questions. Since this study aims in comparing the understanding of participants when using both our tool and Paraview to complete a task, we asked them to fill in an additional form to know their background in Scientific Visualization and Paraview.

**TABLE 3. Study 2 participants demographic.**

Gender	
Male	2
Female	5
Age	
18-25	6
26-35	1
Currently pursuing/graduated from CS background?	
Yes	2
No	5
Currently working in CS related field?	
Yes	1
No	6

**TABLE 4. Time needed to complete the "Find-the-Lobster" task using our tool versus Paraview's transfer function feature (\*were given hint one time to complete the task; \*\*were given hints two times to complete the task).**

	Using Our Tool	Using Paraview
User-1	00:28.9	00:53.0
User-2	00:16.7	01:04.5*
User-3	00:30.5	01:02.7
User-4	00:15.9	00:47.1
User-5	00:08.4	00:20.5
User-6	00:52.9*	02:49.0**
User-7	00:12.1	00:21.5
<b>Average</b>	<b>00:23.6</b>	<b>01:02.6</b>

After filling out the forms, participants are then first shown our tool. The participants are then explained the basics of the tool by letting them watch a 2-minute and 20-second video. This video is the same as the one used in study 1 and it discussed the goal of the tool, the menu interface, and various features that the tool has. After watching the introduction of our tool, they are asked to complete the "Find-the-Lobster" task.

After the participants completed the task using our tool, they were shown the Paraview tool. Same to the first half of the study, the participants are then given information about how to use Paraview. This information is provided in the form of a 2-minute and 24-second tutorial video which is of similar length to our tool's introduction video. We focused on explaining transfer function and volume rendering since those are the two topics that are related to the task. Participants are urged to complete the task on their own, but they are allowed to ask questions and ask for further explanation for Paraview's features related to the task. Participants can also end the task by giving up; in that case, the researcher will provide them with the answers.

After completing both the task using our tool and Paraview, the participants are asked for semi-structured interviews to compare the usage of both tools.

### 3) RESULTS

We analyze the results of the task completed using either our tool or Paraview. As shown in figure 4, all participants were able to complete the task using our tool faster than using the Paraview. The average time to finish the task using our

tool is 23.6 seconds, with the fastest speed of 8.4 seconds and the slowest at 52.9 seconds. While it takes on average 1 minute and 2.6 seconds to complete the same task using Paraview's transfer function feature, with 20.5 seconds being the fastest and 2 minute and 49 seconds the slowest. The average difference in the time needed to complete the task with our tool and Paraview is 40 seconds. Table 4 shows that when using our tool to complete the task, only one participant (14.3%) asked for hints. In contrast, two (28.6%) participants asked for further explanation or hints when trying to use Paraview's transfer function features to do the same task.

We predict the potential reason for this is because of two things: easier to understand without a lot of prior knowledge and our tool's simplicity compared to Paraview. When trying to remove occlusion from a 3D object, using our tool's feature, users can click to remove the obstruction while using the transfer function feature in Paraview, users need to at least know how the buttons in the transfer function feature affect the visualization. Six out of seven participants (85.7%) have no prior knowledge of scientific visualization and thus they also have no background in volume rendering and transfer function.

When completing the task using our tool, they were able to understand the tool enough that they knew what to do when trying to complete the task. When asked to do the task, six (85.7%) participants were able to do it right away and five (71.4%) of them were able to state the answer using both features that our tool has. While only one (14.3%) participant asked for hints to finish the task. In completing "Find-the-Lobster", five (71.4%) participants prefer to use the (Global) Erasing Structure. User7 provides an explanation "since I don't know where the location of the lobster is, I need more time with the digging mode because I have to first find the location of the lobster so it is safer to use the other mode".

On the other hand, there are more participants asking for hints when trying to complete the task using Paraview. Some participants would count on trial-and-error and basically brute-forcing their way to complete the task. User3 said that "Until the very end, I still don't know how it (transfer function feature) works. I just keep pressing buttons until something works".

When comparing both tools to complete the task, all of the participants stated that our tool is easier to use than Paraview's transfer function tool. User5 said that "When trying to complete the task using this tool (our tool), I only need to know that pressing the layer will remove it and give me the layer underneath it. With the Paraview tool, I need to know what the purple-white thing (the buttons in Paraview's transfer function feature) means". Four (57.1%) of participants also explicitly stated that our tool is simple enough and was able to easily connect the meaning when clicking and how it affects the visualization. User2 further elaborates by saying "In my opinion, I can understand this tool (our tool) better. Like, I understand clicking this (the 3D object structure in our tool) will remove the part and show the layer inside. For Paraview, I understand that dragging this (the transfer

function button) will change the transparency of the object but I don't know how much it changes or why this (a part of the teapot visualized) cannot go away when I drag the button."

Another thing that we suspect contributes to our tool being considered better than Paraview by the participants is the simplicity of our tool. User1 mentioned that "(using our tool) you just need to click (the object) and the layer is gone, it's super simple. When using the other tool (Paraview) and I sometimes do this (drag the transfer function feature button which is located in the blue part) I expect this part (the blue part of the object) to be gone but no the other part is gone instead". Our tool's simplicity and easiness to use are also backed up by the result of study 1 which used the SUS. Our tool gains an average score of 8.3 out of 10 for question 3 (I thought the system was easy to use), and also an average of 8.2 out of 10 for question 2 (I don't find the system unnecessarily complex).

Although our evaluation shows that our tool is simpler and easier to use, we recognize that our tool could not be the best choice if users want to conduct a rigorous data exploration. User4, a current undergraduate student majoring in Computer Science and has used Paraview before, stated that "It took me faster using your tool because there are only two modes that I need to consider. When you first told me to complete the task using Paraview, I was considering a few options that I can do to complete it with Paraview but since there are so many features, it took me a while.". When asked which tool they prefer to use, user4 also adds that "This (our tool) is simpler to use. If I just want to see the different layers, I would choose your tool. But if I want to find something more detailed, I think Paraview is still better.". From user4's viewpoint, Paraview is still a more powerful visualization tool, but our tool is highly user-friendly, particularly for less complex tasks.

## VII. DISCUSSION

This section discusses the impact of the transfer function and the number of material structures configuration on the non-expert data exploration.

### A. MATERIAL NUMBERS

When the data providers set up the dataset, our system divides the dataset into  $N$  material structures by the approach introduced in Sec. III-A. By our approach, the data providers can choose the parameter  $N$ . If the number of  $N$  is too small, one click from non-expert users could remove too much portion of the dataset that consists of multiple materials, such as removing bone and muscle with just one click. If the  $N$  is large, the non-expert users can explore the data with more detail because only a thin layer is dug out after one click. However, compared to a relatively small  $N$  configuration, the users will spend much more time removing the same obstructing structure. In addition, dividing a structure into more layers could provide improper context and increase the difficulty for users to understand the dataset. The foot dataset shown in Fig. 12 is an example. If the data providers set a larger number of  $N$  (Fig. 12(b)), the muscle is divided into

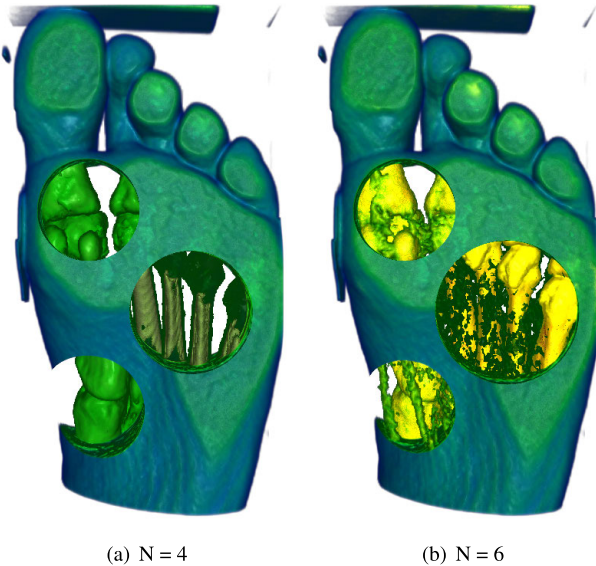


**FIGURE 12.** The difference after the digging out action on the same dataset if the data provider sets different number of material structures.

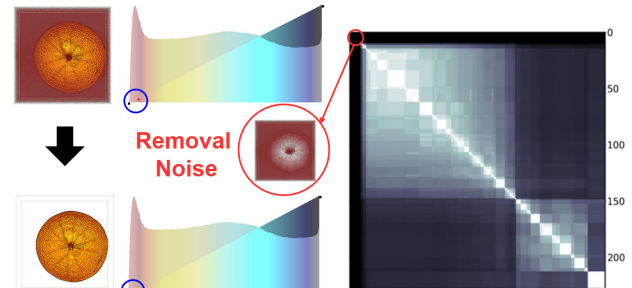
multiple layers. If the non-expert users intend to remove the muscle, a portion of the muscle material will remain, and the image cannot provide a clear boundary.

#### B. TRANSFER FUNCTION DESIGN

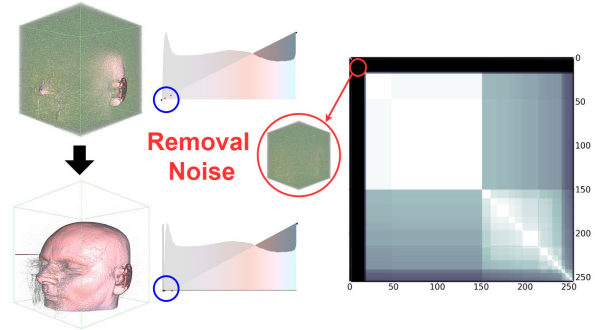
Our system shows the isovalue similarity heatmap for data providers to select representative structures in groups. The diagonal line of the isosurface similarity heatmap displays the similarity value of self-isosurfaces. Typically, the diagonal value should be 1. After determining the number of material structures, the data provider can assign transfer functions (opacity and color) to each material structure. A data volume is a cube, and the region of interest of the dataset usually does not cover the whole cube. For example, a large outer region of the head dataset shown in Fig. 13 is an empty space, and the non-expert users may not be interested in that region. Non-expert users do not have to observe and dig out this region. The data provider can recognize this region in the isovalue similarity heatmap and set the opacity of this data value range to 0, and make it invisible. In this manner, the empty space that impacts the non-expert users' observation volume data during volume rendering can be filtered out in the beginning.

#### C. SOFTWARE IMPLEMENTATION

The system was implemented using C# and HLSL programming languages in Unity3D. In order to perform pre-computations of material structures, we developed a custom implementation using Python. For the implementation of the convex parts, we utilized the V-HACD library [43]. In order to conduct the case and user studies, participants were given the option to either visit our laboratory or use the tool at home. Therefore, the software was developed on both Windows and MacOS to accommodate a diverse pool of participants. The software, sampled datasets, tuto-



(a) Orange Dataset.



(b) MRI-Head Dataset.

**FIGURE 13.** The empty space removal in the initial volume rendering results through the data providers' transfer function configuration for non-expert users to start the data exploration without the meaningless empty space occlusion.

rial and demonstration video can be downloaded from our Github repository ([link here](#)). The current implementation was designed for conducting user studies and will require adaptation to deploy to the target environment, such as a science museum. In the future, the implementation should be modified to support the use of high-resolution touch screens and tablet operating systems, such as iOS.

#### VIII. CONCLUSION AND FUTURE WORKS

In this paper, we first analyze the shape similarity of the material structures to enable the data provider to adjust the material's color and opacity. This will help the data provider in creating a more comprehensible dataset for non-expert users to navigate during data exploration. We then propose progressive digging interaction modes that mimic digging behavior to allow non-expert users to easily explore the data. We also developed a comprehensive, interactive interface that enables users to adjust the changes in material structure, lens size, and shape. Our tools are then evaluated by two studies. The first study explores the tool's and features usability with System Usability Scale (SUS) and additional questions focusing on the tool's digging modes and the second study compares our tool with another tool. We also held interviews to gain a further understanding of the participant's answers in both studies. On the SUS scale, our tool has a score of 76.7 which meant that our tool can be considered good or has high usability by the participants. From the SUS score

results and interviews, we can also conclude that our tool can be easily used for non-expert users which are our target audience. In the future, we will extend our system to more scientific data types, such as particle and vector datasets

## REFERENCES

- [1] R. A. Drebin, L. Carpenter, and P. Hanrahan, "Volume rendering," *SIGGRAPH Comput. Graph.*, vol. 22, no. 4, pp. 65–74, Jun. 1988.
- [2] C. Hurter, A. R. Taylor, S. Carpendale, and A. Telea, "Interactive exploration and selection in volumetric datasets with color tunneling," in *Proc. 27th Annu. ACM Symp. User Interface Softw. Technol.*, 2014, pp. 49–50.
- [3] Y. Wu and H. Qu, "Interactive transfer function design based on editing direct volume rendered images," *IEEE Trans. Vis. Comput. Graph.*, vol. 13, no. 5, pp. 1027–1040, Sep. 2007.
- [4] R. Huang and K.-L. Ma, "RGVis: Region growing based techniques for volume visualization," in *Proc. 11th Pacific Conf. Comput. Graph. Appl.*, 2003, pp. 355–363.
- [5] W. E. Lorensen and H. E. Cline, "Marching cubes: A high resolution 3D surface construction algorithm," *ACM SIGGRAPH Comput. Graph.*, vol. 21, no. 4, pp. 163–169, Aug. 1987.
- [6] C. D. Correa, "Illustrative Deformation of volumetric objects and other graphical models," Ph.D. thesis, Rutgers, State Univ. New Jersey, New Brunswick–Piscataway, NJ, USA, 2007, doi: [10.7282/T3WH2QFM](https://doi.org/10.7282/T3WH2QFM).
- [7] Å. Birkeland and I. Viola, "View-dependent peel-away visualization for volumetric data," in *Proc. 25th Spring Conf. Comput. Graph.*, Apr. 2009, pp. 121–128.
- [8] M. J. McGuffin, L. Tancau, and R. Balakrishnan, "Using deformations for browsing volumetric data," in *Proc. IEEE Visualizat.*, Mar. 2003, pp. 401–408.
- [9] C. Li, "Interactive data deformation techniques to improve feature visibility in scientific visualization," Ph.D. thesis, Dept. Comput. Sci. Eng., Ohio State Univ., Columbus, OH, USA, 2018.
- [10] M. Traoré, C. Hurter, and A. Telea, "Interactive obstruction-free lensing for volumetric data visualization," *IEEE Trans. Vis. Comput. Graph.*, vol. 25, no. 1, pp. 1029–1039, Jan. 2019.
- [11] S. Stoppel and S. Bruckner, "Smart surrogate widgets for direct volume manipulation," in *Proc. IEEE Pacific Visualizat. Symp. (PacificVis)*, Apr. 2018, pp. 36–45.
- [12] C. Xu, G. Sun, and R. Liang, "A survey of volume visualization techniques for feature enhancement," *Vis. Informat.*, vol. 5, no. 3, pp. 70–81, Sep. 2021.
- [13] B. Ma and A. Entezari, "Volumetric feature-based classification and visibility analysis for transfer function design," *IEEE Trans. Vis. Comput. Graph.*, vol. 24, no. 12, pp. 3253–3267, Dec. 2018.
- [14] C. Y. Ip, A. Varshney, and J. JaJa, "Hierarchical exploration of volumes using multilevel segmentation of the intensity-gradient histograms," *IEEE Trans. Vis. Comput. Graph.*, vol. 18, no. 12, pp. 2355–2363, Dec. 2012.
- [15] Y. Wang, J. Zhang, W. Chen, H. Zhang, and X. Chi, "Efficient opacity specification based on feature visibilities in direct volume rendering," *Comput. Graph. Forum*, vol. 30, no. 7, pp. 2117–2126, Sep. 2011.
- [16] C. D. Correa and K.-L. Ma, "Visibility histograms and visibility-driven transfer functions," *IEEE Trans. Vis. Comput. Graph.*, vol. 17, no. 2, pp. 192–204, Feb. 2011.
- [17] C. E. Shannon, "A mathematical theory of communication," *Bell Syst. Tech. J.*, vol. 27, no. 3, pp. 379–423, Jul. 1948.
- [18] S. Bruckner and T. Möller, "Isosurface similarity maps," in *Proc. IEEE-VGTC Symp. Visualizat.*, Jan. 2010, pp. 773–782.
- [19] T.-H. Wei, T.-Y. Lee, and H.-W. Shen, "Evaluating isosurfaces with level-set-based information maps," *Comput. Graph. Forum*, vol. 32, no. 3, pp. 1–10, Jun. 2013.
- [20] N. Elmqvist and P. Tsigas, "A taxonomy of 3D occlusion management for visualization," *IEEE Trans. Vis. Comput. Graph.*, vol. 14, no. 5, pp. 1095–1109, Sep. 2008.
- [21] J. Cui, P. Rosen, V. Popescu, and C. Hoffmann, "A curved ray camera for handling occlusions through continuous multiperspective visualization," *IEEE Trans. Vis. Comput. Graph.*, vol. 16, no. 6, pp. 1235–1242, Nov. 2010.
- [22] M.-L. Wu and V. Popescu, "Multiperspective focus+context visualization," *IEEE Trans. Vis. Comput. Graphics*, vol. 22, no. 5, pp. 1555–1567, May 2016.
- [23] C. Tominski, S. Gladisch, U. Kister, R. Dachselt, and H. Schumann, "Interactive lenses for visualization: An extended survey," *Comput. Graph. Forum*, vol. 36, no. 6, pp. 173–200, Sep. 2017.
- [24] C. Correa, D. Silver, and M. Chen, "Feature aligned volume manipulation for illustration and visualization," *IEEE Trans. Vis. Comput. Graph.*, vol. 12, no. 5, pp. 1069–1076, Sep. 2006.
- [25] C. Li, X. Tong, and H.-W. Shen, "Virtual retractor: An interactive data exploration system using physically based deformation," in *Proc. IEEE Pacific Visualizat. Symp. (PacificVis)*, Apr. 2017, pp. 51–60.
- [26] C. Li and H.-W. Shen, "Object-in-hand feature displacement with physically-based deformation," in *Proc. IEEE Pacific Visualizat. Symp. (PacificVis)*, Apr. 2019, pp. 21–30.
- [27] C. Lundstrom, T. Rydell, C. Forsell, A. Persson, and A. Ynnerman, "Multi-touch table system for medical visualization: Application to orthopedic surgery planning," *IEEE Trans. Vis. Comput. Graph.*, vol. 17, no. 12, pp. 1775–1784, Dec. 2011.
- [28] F. Marton, M. B. Rodriguez, F. Bettio, M. Agus, A. J. Villanueva, and E. Gobbetti, "IsoCam: Interactive visual exploration of massive cultural heritage models on large projection setups," *J. Comput. Cultural Heritage*, vol. 7, no. 2, pp. 1–24, Jun. 2014.
- [29] F. Murtagh and P. Contreras, "Algorithms for hierarchical clustering: An overview," *WIREs Data Mining Knowl. Discovery*, vol. 2, no. 1, pp. 86–97, Jan. 2012.
- [30] A. Wiebel, F. M. Vos, D. Foerster, and H.-C. Hege, "WYSIWYP: What you see is what you pick," *IEEE Trans. Vis. Comput. Graph.*, vol. 18, no. 12, pp. 2236–2244, Dec. 2012.
- [31] K. Mamou and F. Ghorbel, "A simple and efficient approach for 3D mesh approximate convex decomposition," in *Proc. 16th IEEE Int. Conf. Image Process. (ICIP)*, Nov. 2009, pp. 3501–3504.
- [32] D. Le Vay, J. S. Robson, and G. A. G. Mitchell. (2020). *Renal System*. Accessed: Sep. 10, 2022. [Online]. Available: <https://www.britannica.com/science/human-renal-system>
- [33] The Editors of Encyclopaedia Britannica. (2022). *Rutherford Model*. Accessed: Sep. 10, 2022. [Online]. Available: <https://www.britannica.com/science/Rutherford-model>
- [34] J. Ahrens, B. Geveci, C. Law, C. Hansen, and C. Johnson, "ParaView: An end-user tool for large-data visualization," in *The Visualization Handbook*, vol. 717, 2005, p. 50038–1.
- [35] CIBC. (2016). *ImageVis3D: An Interactive visualization Software System for Large-Scale Volume Data*. Scientific Computing and Imaging Institute (SCI). [Online]. Available: <http://www.imagevis3d.org>
- [36] J. Brooke, "SUS-A quick and dirty usability scale," *Usability Eval. Ind.*, vol. 189, no. 194, pp. 4–7, 1996.
- [37] N. A. Nik Ahmad and P. N. N. Megat Sazali, "Performing user acceptance test with system usability scale for graduation application," in *Proc. Int. Conf. Softw. Eng. Comput. Syst. 4th Int. Conf. Comput. Sci. Inf. Manage.*, Aug. 2021, pp. 86–91.
- [38] Y. Wang, T. Lei, and X. Liu, "Chinese system usability scale: Translation, revision, psychological measurement," *Int. J. Hum.-Comput. Interact.*, vol. 36, no. 10, pp. 953–963, Jun. 2020.
- [39] A. Joshi, S. Kale, S. Chandel, and D. Pal, "Likert scale: Explored and explained," *Brit. J. Appl. Sci. Technol.*, vol. 7, no. 4, pp. 396–403, Jan. 2015.
- [40] J. R. Lewis and J. Sauro, "Item benchmarks for the system usability scale," *J. Usability Stud.*, vol. 13, no. 3, pp. 1–10, 2018.
- [41] J. R. Lewis and J. Sauro, "The factor structure of the system usability scale," in *Proc. Int. Conf. Hum. Centered Design*. San Diego, CA, USA: Springer, Jul. 2009, pp. 1–12.
- [42] U. Ayachit. *The Paraview Guide: A Parallel Visualization Application*. Clifton Park, NY, USA: Kitware, 2015.
- [43] K. Mammou. *V-HACD Library*. Accessed: Sep. 10, 2022. [Online]. Available: <https://github.com/kmammou/v-hacd>



**JING-RU SUN** received the M.S. degree in computer science and information engineering from National Taiwan Normal University, in 2022. Her research interests include analysis and visualization of volume data and interactive visualization.



**NATHANIA JOSEPHINE** received the B.S. degree in computer science and information engineering from National Taiwan Normal University, Taipei, Taiwan, in 2022, where she is currently pursuing the M.S. degree in computer science and information engineering. Her research interests include data visualization and data analysis.



**KO-CHIH WANG** (Member, IEEE) received the Ph.D. degree in computer science from The Ohio State University. He is currently an Assistant Professor with National Taiwan Normal University, Taipei, Taiwan. His research interests include large-scale scientific data visualization, visual analytics, computer graphics, and high-performance computing.

• • •



**CHAO WANG** (Member, IEEE) received the B.S. degree in electrical engineering and the M.S. degree in computer and communication engineering from National Cheng Kung University, in 2009 and 2010, respectively, and the Ph.D. degree in computer science from Washington University in St. Louis, in 2019. He is currently an Assistant Professor with the Department of Computer Science and Information Engineering, National Taiwan Normal University. His research interest includes studying cyber-physical systems. He is a member of ACM.